Available online at www.sciencedirect.com
SCIENCE DIRECT®
Journal of Nuclear Materials 336 (2005) 217–224
journal of nuclear materials
www.elsevier.com/locate/jnucmat

Radiation swelling behavior and its dependence on temperature, dose rate, and dislocation structure evolution

Michael P. Surh, J.B. Sturgeon *, W.G. Wolfer

Lawrence Livermore National Laboratory, Livermore, CA 94550, USA

Received 2 February 2004; accepted 17 September 2004

Abstract

The microstructural evolution of high-purity steel under irradiation is modeled including a dislocation density that evolves simultaneously with void nucleation and growth. Analysis of the coupled microstructure sinks indicates the evolving dislocation density shapes the rate of void nucleation and the void size distribution so as to enhance steady-swelling behavior at high doses. The incubation dose, to roughly the point of transition to steady-state swelling, is closely related to and even controlled by evolution of the dislocation structure. Incubation is thus a strong function of both the irradiation temperature and the dose rate. The predicted swelling trends versus temperature, flux, and time are closer to experimental results than earlier calculations of void nucleation and growth with a fixed dislocation density.

1. Introduction

Irradiation-induced swelling in reactor steels commonly exhibits an incubation period during which the volume change initially remains small despite the increasing radiation dose. The duration of this incubation stage depends on temperature, dose rate, and initial characteristics like dislocation density and solute concentrations [1–7]. Eventually, the swelling rate accelerates to a value around 1%/dpa (displacement per atom) for austenitic stainless steels. Once achieved, this rate is fairly constant over many subsequent dpa of irradiation. It is also largely independent of temperature and flux over wide ranges.

Microscopically, all aspects of this evolution are driven by competition among dislocations, defect clusters, and stable voids for the mobile defects created by damage cascades. Much of the radiation damage subsequently annihilates, but some portion contributes to persistent changes in the material, including swelling. Stress-mediated interactions between defects lead to a preferential segregation of interstitials (or mobile interstitial clusters) at climbing dislocations, and a corresponding net influx of vacancies at growing voids and vacancy clusters [8–10]. Swelling does not occur absent growing voids because dislocations then absorb equal numbers of vacancies and interstitials on average.

Accurate modeling of this annihilation/segregation behavior demands a self-consistent treatment of the total defect population including the deposition of new defects by irradiation and the results of mutual reactions within the population. A complete account of the radiation damage process should also include for the

* Corresponding author.
E-mail address: jsturgeon@llnl.gov (J.B. Sturgeon).

0022-3115/$ - see front matter © 2004 Elsevier B.V. All rights reserved.
doi:10.1016/j.jnucmat.2004.09.016

heterogeneous distribution of the cascade debris. For example, cascade simulations indicate that interstitial clusters are mostly deposited in a halo around a central distribution of vacancy clusters [11]. In contrast, early models of swelling deposit radiation damage as isolated defect monomers and then solve mean-field reaction rate equations for a simplified system of supersaturated defect monomers, stable, TEM-visible voids, and dislocations [8,12,13]. We will refer to this approach as the 'standard' rate theory. These standard rate theories have not been entirely successful at reproducing experiment, and it is widely believed that their principal shortcoming is the neglect of defect clustering within the cascade, before any reactions occur with the pre-existing microstructure [14,15]. Other suggested limitations include that the mean field approximation does not account for persistent spatial variations such as inhomogeneous microstructure [13], or that there are additional fluctuations in mobile defect densities due to cascade damage deposition events [16].

However, uncontrolled mathematical approximations have also been introduced into these models, besides various assumptions about microscopic processes. These numerical deficiencies may instead account for discrepancies with experiment. For example, some early solutions of the rate equations preclude any fluctuations in cluster size. That is to say that like-sized clusters grow or shrink in lock-step, remaining like-sized at all later times [8,12,13,17]. This continuous, deterministic evolution is not a requisite of the mean field approximation. Master equation approaches [18] employ mean field reaction rates, but account for temporal fluctuations in cluster size. Similarly, time-dependent fluctuations are automatically included in the Fokker–Planck formalism [18–20]. Whether or not the mean field approximation is justified in cascade damage conditions; continuous, deterministic evolution is known to be a poor approximation for small clusters [19].

Yet other uncontrolled approximations are commonly made by truncating the void size distribution in rate theories of radiation damage [8,12,13,17]. The aforementioned standard rate theory models ignore the effect of sub-critical defect clusters entirely. This gives an additional shortcoming; such models cannot provide a self-consistent treatment of the nucleation of stable voids. Standard rate theories with truncated void size distributions (monomers plus stable voids) may be solved (internally) self-consistently, but they are never self-consistent theories of vacancy aggregation or void nucleation. More recent models assume that these clusters arise from the initial clustering of the defects within the cascades, exclusive of the monomer aggregation that drives the growth of large clusters [21]. These models introduce stable voids by fiat (e.g., in accord with experimental measurements) or by some plausible but limited process. A self-consistent theory requires that the entire population of vacancy clusters of all sizes be treated together with the monomer (and any other mobile) reactants, without artificial approximations as to the distribution or range of cluster sizes or as to the reaction pathways leading to stable clusters. Rate equations for vacancy absorption at large voids cannot be examined in isolation from vacancy absorption at small voids or even in isolation from direct vacancy-vacancy aggregation. (Obviously, non-equilibrium dimer and sub-critical cluster formation is an inevitable consequence of a vacancy supersaturation. No fully self-consistent treatment of cluster evolution can neglect this process, without first proving that it is negligible.) At the very least, by failing to include the presence of sub-critical clusters, standard rate theory models will fail to describe transient behavior at the onset of irradiation, when mostly vacancies plus small voids are present [13].

Finally, while a recent Fokker–Planck study [21] accounts for most sub-critical clusters, it does not appear to be self-consistent. The study calculates cluster evolution rates assuming a time-independent vacancy and interstitial concentration. In actuality, the monomer concentrations rapidly adapt to reflect changes in the aggregate sink strengths of the material microstructure. Thus, the conditional probabilities in the integrands of Eqs. (12) and (14) in Ref. [21] are themselves functional of the entire, time-dependent defect cluster size distribution. The need for self-consistency imposes strict requirements on any numerical solution. The density of mobile monomers adapts rapidly, so the coupled rate equations are stiff. This feature demands careful treatment of the numerical evolution [22,23], or a scheme for treating the monomers separately from the rest of the system [18,19]. In addition, the exclusion of vacancy dimers and trimers in [21] introduces an uncontrolled approximation into the evolution equations. Older, classical nucleation theories include all sub-critical cluster sizes, but similarly assume a time-independent concentration of monomers [9,24], and so are not self-consistent, either.

Given widespread misconceptions about the validity of early rate theory approximations, it is entirely unclear what the pre-dominant shortcomings are in the existing numerical solutions. As a first step, accurate, complete solutions of the mean field rate equations should be obtained. A variety of improvements, modifications, or embellishments may then be examined, in turn. Recently, simulations of void evolution and irradiation swelling behavior have been analyzed for a model with a constant dislocation density [18]. This simplification allowed study of void nucleation and growth in isolation from other, concurrent changes in the microstructure. This was the first completely self-consistent treatment to high dose of any model of vacancy aggregation in metals, the void size distribution being neither arbitrarily truncated nor artificially initialized. The model suc-

cessfully reproduced transient incubation-like behavior followed by quasi-steady swelling. Based on these results, at least part of the incubation behavior may be identified with the development of large, stable voids, supporting the use of nucleation and growth simulations [19,25,26] for transient swelling behavior. Significantly, a good part of the incubation behavior could be reproduced without invoking preformed defect clusters within the cascade of initial atomic displacements.

While such calculations give a plausible incubation [18,27], they fail to reproduce other qualitative features of experimental swelling. For example, much of the acceleration of swelling during the experimental incubation period occupies only a fraction of its duration, towards the end of the interval. In general, those experiments with the longest incubation delays exhibit the sharpest crossover to steady swelling [1]. In contrast, the predicted swelling was found to rise smoothly during incubation. The longest predicted delays were the most gradual, where swelling exhibited a power-law behavior versus time [27]. Additionally, while the experimental swelling appears to be steady after incubation [1], the predicted swelling rate declined with time. (The calculated peak rate could fall by half at 100 dpa [27].) Finally, the experimental steady-swelling rates are largely independent of temperature and flux over wide ranges [1]. In contrast, the simulated swelling was visibly dependent on the temperature and dose rate. The predicted swelling curves at different temperatures tended to cross one another because the longer incubation cases seemed to lead to higher peak swelling rates [27]. The calculated incubation delays were very short, more consistent with experiments on high-purity steel, but the observed flux-dependence suggests that another process in the overall microstructural evolution (besides void nucleation and growth) must be involved.

It is well known that dislocation densities simultaneously evolve with the voids under irradiation bombardment. The resulting time-dependent changes in the dislocation sink strength will influence the predicted swelling behavior. Thus, co-evolution of dislocations must be included along with the careful modeling of voids when comparing rate-theory simulations to observations. More realistic simulations of time-dependent dislocation and void populations have recently been performed, and a preliminary examination of a combined dislocation/void evolution model shows encouraging results for swelling behavior [28].

In this paper, we report further on simulations of void and dislocation co-evolution. We model a pure austenitic stainless steel, with a starting dislocation density of $6 \times 10^{13}\,\mathrm{m}^{-2}$, corresponding to a solution annealed condition. We examine incubation doses, quasi-steady-swelling rates, and terminal void and dislocation densities and their dependence on temperature, flux, and dose. This co-evolution model does not include preformed defect clusters. There are no separate interstitial clusters or dislocation loops and no explicit loop formation or coalescence, although these processes are implicit in the dislocation evolution model. This is not to argue that such phenomena are not prominent in an irradiated material, since loops are clearly visible in experiments. The calculations presented here reveal how void nucleation and dislocation evolution can be critical factors in the swelling of irradiated materials, but do not exclude other processes from contributing. Having said this, the qualitative successes of the co-evolution model suggest that swelling behavior may not be so strongly influenced by cascade defect clustering.

The full set of simulations reveals how the sink strengths of dislocations and voids change self-consistently with the mobile defect population and thus depend on environmental parameters like temperature and flux. The transient formation of many small clusters, their occasional growth to stable size, the subsequent decrease of the sub-critical population, and yet its overall persistence even after nucleation is complete, all influences the macroscopic swelling behavior. The final density of (stable, visible) voids depends on the initial dislocation density, besides environmental parameters. The terminal dislocation density is mainly a function of temperature and flux and the final void density; it is not directly dependent on the original dislocation content. Unstable or sub-critical clusters never reach a truly constant concentration; they are sustained at some elevated concentration by the evolving vacancy supersaturation (itself a function of the environment and the evolving void and dislocation content). The competition among these three temperature-, flux-, and time-dependent sinks nevertheless creates a nearly constant swelling rate at about 1%/dpa for a wide range of conditions. To understand this result, the flow of radiation-induced defects is analyzed by comparing total sink strengths of the dislocations and voids. Based on this analysis, the improved agreement with experiment as compared to our earlier results [18] may be attributed to a reduced nucleation of voids in the solution-annealed material, followed by an increase of dislocation density (dislocation sink strength) by approximately an order of magnitude.

2. Time-dependent dislocation model

During irradiation, dislocation evolution depends on thermal annealing processes, a net influx of radiation-induced defects to pre-existing dislocations, and on loop nucleation, loop growth, and loop coalescence into the dislocation network. The overall behavior has been examined in an earlier study, assuming that dislocation segments in the initial network experience a range of different local environments which affects their bias factor

[29]. With one free parameter, the model obtains reasonable results for the total dislocation density, ρ, versus temperature, time, and irradiation flux as compared to experiment. The result is expressed with separate annihilation and production processes by the equation:

$$\frac{d\rho}{dt} = -A\rho^2 + B\rho. \quad (1)$$

The quadratic term in Eq. (1) is consistent with dislocation dipole annihilation. Its pre-factor is obtained from a detailed model for the rate of dipole annihilation under combined glide and climb of dislocation segments. Segment motion is driven both by thermal annealing and by the non-equilibrium flux of mobile defects due to irradiation. Individual dislocation segments receive different fluxes of vacancies or interstitials (even in the absence of voids) because the local environments and bias factors of the dislocation segments are assumed to vary by random amounts. The separate term for production of dislocation segments, $B\rho$, models the process as dislocation bowing between pinning points under the net supersaturation of defects (the linear dependence being consistent with production at Bardeen–Herring sources). These curved dislocation segments also serve to incorporate loop growth into the model in an approximate manner. The pre-factor depends on an average separation of pinning points, l (which is the only adjustable parameter). This parameter is fit to the measured terminal dislocation density at some temperature and dose rate. Ultimately, segment annihilation (creation) is not simply quadratic (linear) in the density, since the coefficients, A and B, are also functionally dependent on ρ.

It had originally been assumed in the development and application of this dislocation model that the void sink strength remains constant over time. This restriction has been lifted in the present implementation, resulting in a dislocation evolution which couples self-consistently to the void evolution [28]. The time-dependent defect flux to dislocations is proportional to the instantaneous monomer concentrations, and so depends indirectly on the sink strength for the co-evolving voids, as well.

The computational method for treating void evolution has been previously described in detail [18]. Vacancy clusters are taken to be spherical sinks, and the cross-section for monomer impingement taken to be proportional to the sum of cluster and vacancy radii. Stress-induced interactions and bias factors for voids and dislocations are calculated in the mean field treatment. Thermal vacancy emission rates are obtained from a fit to cluster energies and detailed-balance arguments. Cluster growth and evaporation are treated stochastically, to capture the nucleation of stable clusters including transient behavior.

Vacancy and interstitial concentrations are calculated in a quasi-stationary approximation, assuming that all irradiation damage is introduced as defect monomers and including the sink strength of the voids and dislocations in the usual mean field approximation. Dislocations are modeled as straight network segments at a given density for purposes of the computing the biased dislocation sink strengths for monomers. Aggregate void sink strengths are calculated for the full size distribution, including size-dependent bias factors. The entire, coupled system of monomers, dislocations, and voids can be self-consistently evolved to cumulative doses in excess of 100 dpa.

3. Results and analysis

The initial swelling behavior for void and dislocation co-evolution in type-316 stainless steel is shown in Fig. 1. Model parameters are the same as were used for earlier, constant dislocation density simulations. (Representative swelling curves for that model may be seen in Ref. [18].) In the simulations reported here, the swelling curves at multiple temperatures appear to reach the same asymptotic swelling rate, around 0.8%/dpa. The exact value depends on the bias factor model chosen for the dislocations. We recalculate the dislocation bias factors at each time-step to reflect the time-varying dislocation density. The highest temperature case shown (660 °C) is still in the incubation stage at 25 dpa; it increases to a swelling rate of approximately 0.5%/dpa by the end of the simulation at 100 dpa. Incubation periods are visibly much shorter than are seen in commercial

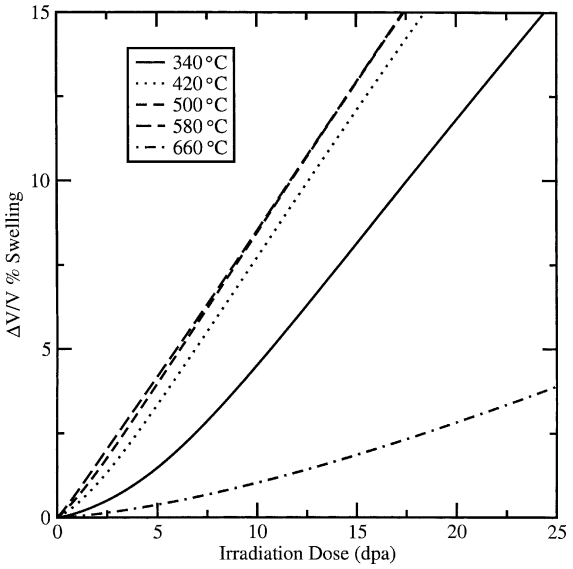

Fig. 1. Volumetric swelling versus dose to 100 dpa for multiple temperatures and for a dose rate of 10^{-6} dpa/s. The temperatures are listed in the figure legend.

reactor steels. However, experiments on high-purity ternary stainless steels have a much shorter incubation delay than commercial steels [3–7]. Such pure materials are closer to our model for precipitate and solute-free steel. Our two principal results, namely, the incubation-like interval followed by steady swelling that is uniform over a range of temperatures, are in good qualitative agreement with the experimental results of Okita et al. [3–7] on pure austenitic alloys.

The predicted crossover from transient to steady swelling is slightly more abrupt now that dislocation evolution is included. The simulations may be numerically differentiated to obtain the swelling rate versus time or dose, shown in Fig. 2, for the full duration of the simulation. There are three changes between the current results and those with a time- independent dislocation model (Ref. [18,27]). First, the swelling takes longer to reach its peak rate. Second, the swelling rate does not always show a single local maximum (versus time), which it invariably does when the dislocation density is held fixed. Finally, the peak swelling rates are better maintained at late times. (For example, the swelling rate at 500 °C remains between 0.7% and 0.9%/dpa from 1 to 100 dpa.)

These differences are all consequences of the evolving dislocation density, which increases from its solution-annealed starting values to a temperature- and flux-dependent terminal value. In a fixed dislocation density model, the voids monotonically grow to become the dominant sinks for vacancies and interstitials. The net swelling rate is initially small when there are few voids present, then increases (incubation behavior) to a maximum value as the stable voids nucleate and grow, and finally declines (quasi-steady behavior) as the void sink strength increases to dominate the dislocations. As this occurs, interstitials increasingly annihilate at the stable voids instead of contributing to dislocation climb, causing the swelling rate to diminish [30]. In contrast, when the dislocation density is allowed to evolve from starting solution-annealed values, the dislocation sink strength also increases monotonically from initial values. The sink strength ratio for voids and dislocations changes more slowly. As a result, the swelling rate can have more than one local extremum, and the peak rate of swelling appears to be better maintained over time. Ultimately, the dislocation density reaches saturation while the voids continue to grow in size. The swelling behavior then resembles the model with a constant dislocation density.

The co-evolution model predicts relatively simple behavior for dislocation and void densities (Figs. 3 and 4). For most (moderate) temperatures, the dislocation density increases from the starting value of $6\times10^{13}\,m^{-2}$. Time-evolution is faster for higher temperatures and dislocation mobility. The terminal dislocation density declines with temperature (for a fixed irradiation rate) as dipole annihilation increases in importance [29]. Visible voids (Fig. 4) nucleate rapidly and reach their approximate terminal densities in fractions of a dpa. Comparing Figs. 3 and 4 demonstrates that void nucleation is completed before the dislocation density changes appreciably. Terminal (stable) void density thus depends on temperature, dose rate, and starting dislocation density, but is independent of terminal dislocation density.

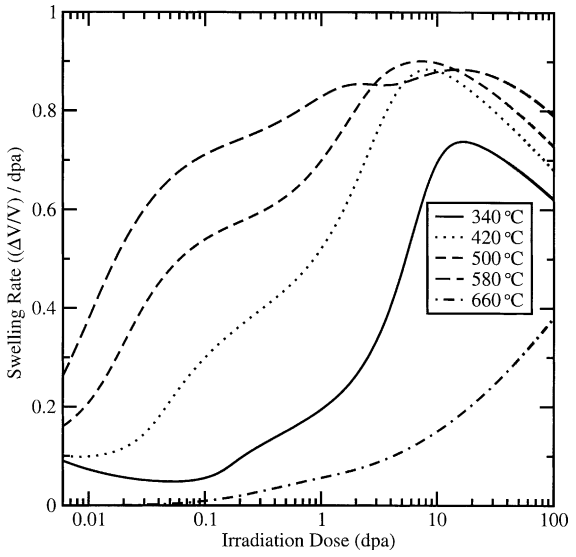

Fig. 2. Swelling rate versus dose for the same temperatures and dose rates as Fig. 1. The roughly straight, declining segments that follow the peaks (e.g., for the curves at 340–580 °C between 20 and 100 dpa) are a characteristic of void sinks that eventually grow to dominate the asymptotic dislocation sinks (see also Fig. 3, Ref. [15]).

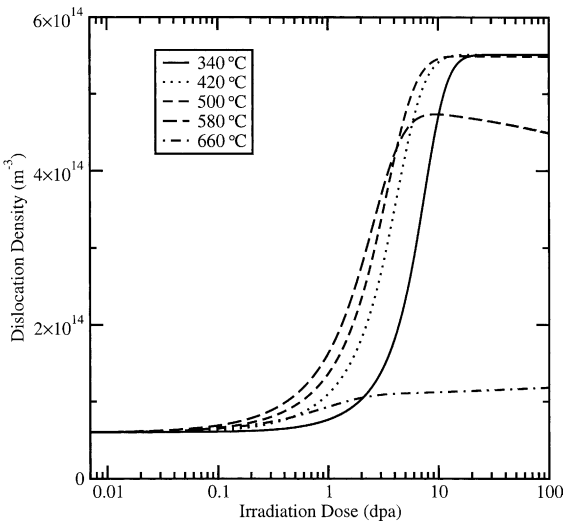

Fig. 3. Dislocation density versus dose for various temperatures and a dose rate of 10^{-6} dpa/s.

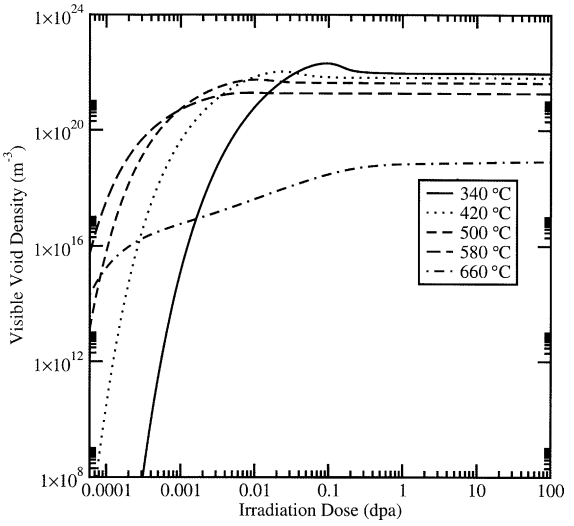

Fig. 4. Visible void density versus dose for various temperatures and a dose rate of 10^{-6} dpa/s. This quantity is a reasonable surrogate for the density of stable voids (i.e., those that continue to grow under the supersaturation of vacancies).

The ratio of the evolving void sink strength to the dislocation sink strength is shown in Fig. 5. A unit ratio is commonly considered to achieve steady swelling, by providing for the most efficient segregation of vacancies and interstitials. The simulations demonstrate that the relative sink strength is essentially never close to unity.

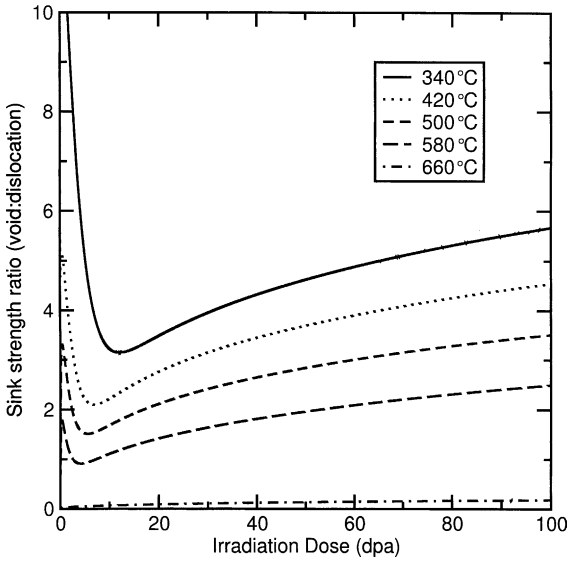

Fig. 5. Ratio of the unbiased sink strengths of voids to dislocations as a function of dose. The void sink strength includes unstable vacancy clusters and vacancy monomers as well as all of the stable voids.

Instead, the ratio transiently reaches large values due to the formation of numerous small, unstable clusters. Here, 'unstable clusters' includes the vacancy monomers as well as small voids. Thus, the unstable cluster sink strength gives a measure of the direct vacancy–interstitial annihilation plus vacancy–interstitial recombination at small vacancy clusters. By the time the vacancy concentration falls and the unstable clusters are reduced in density, the stable voids have grown to provide the dominant sink strength.

Ultimately, the predicted steady-swelling rate lies near 1%/dpa because the underlying defect production rate (0.1 Frenkel pair per dpa) and stress-induced bias factors reproduce the experimentally observed rate of vacancy/interstitial segregation for the high ratio of sink strengths. The swelling is quasi-steady because the defect sinks stay in a narrow post-incubation range (near 2:1 to 4:1) for the length of the simulation and for a wide range of temperature. Two factors help preserve this ratio. First, for most temperatures, fewer stable voids nucleate when the initial dislocation content is low (see Fig. 12, Ref. [27]). Thus, for a given amount of swelling, solution-annealed initial conditions yield fewer, larger stable voids. This better preserves the ratio of sink strengths over subsequent volume changes. (This effect is easily understood: Once stable voids have finished nucleating, swelling increases their average volume essentially in proportion to the macroscopic volume change. However, sink strengths increase proportionally to the void radius. Thus, the total change in void sink strength for a given volume change is less if there are few, large voids in the system with initial aggregate volume ΔV_1 that grow to ΔV_2 than if there are many, small voids which grow from ΔV_1 to ΔV_2.) Second, the solution-annealed dislocation density increases to a terminal value (typically by a factor of 10) after the stable voids have nucleated. This makes the ratio of sink strengths even less sensitive to the continuing void growth and thereby prolongs the quasi-steady-swelling behavior.

For example, the decrease from the peak rate in the log-linear plots from Fig. 2 (e.g., for 340–580 °C) have approximately the same slope as Fig. 2 in Ref. [27]. However, the peak is here achieved much later (near 10 dpa instead of 1 dpa), so the cumulative decrease at 100 dpa is much smaller.

Besides the steady-swelling behavior, we obtain encouraging results on the temperature- and flux-dependent trends in the incubation delay. Fig. 6 shows the predicted incubation time for high-purity austenitic stainless steel as a function of temperature and for three different dose rates. The incubation curves qualitatively resemble simulations where the dislocation density is constrained at the approximate terminal density (6×10^{14} m^{-2}, see Fig. 6, Ref. [27]), although the curves seem to shift to slightly higher temperature here. As before [15], the family of curves in Fig. 6 shows that the

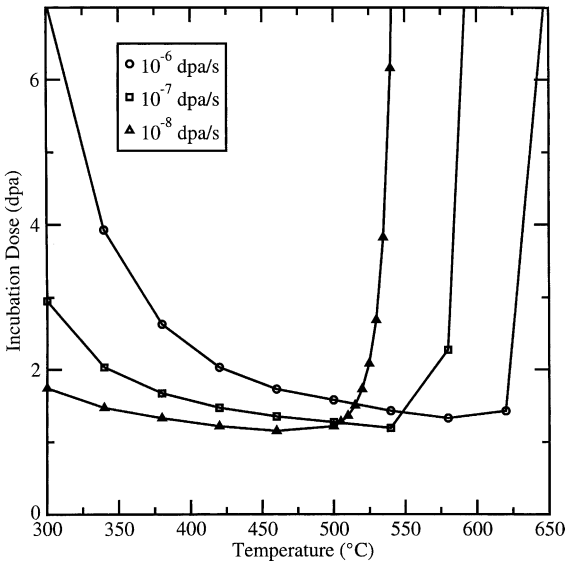

Fig. 6. Incubation dose versus temperature for three irradiation dose rates, of 10^{-6}, 10^{-7}, and 10^{-8} dpa/s. The incubation is defined using a threshold swelling of 1%.

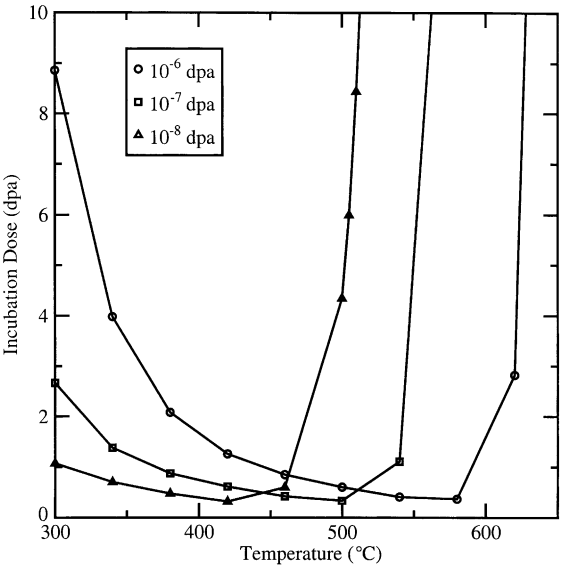

Fig. 7. Incubation dose versus temperature for three irradiation dose rates, of 10^{-6}, 10^{-7}, and 10^{-8} dpa/s. The incubation is defined by linear extrapolation from the point of maximum slope in the swelling curves back to zero swelling.

location of the peak swelling temperature (shortest incubation) shifts to higher temperatures as the flux increases. They also show a so-called dose-rate effect. For moderate temperatures (less than 500–600 °C), the lower flux cases have shorter incubation doses. At higher temperatures, the flux effect mainly acts to shift the upper temperature boundary above which swelling is greatly suppressed.

Fig. 7 displays another definition of the incubation time, namely a linear extrapolation from the steady-swelling portion of the curve back to the abscissa. This definition of incubation gives a stronger dose-rate effect near 400 °C. Experimental measurements on high-purity ternary steel between 408 and 440 °C exhibit a dose-rate effect of the same sign, namely, that the lower flux has the smaller incubation dose [4,5]. However, the experimental dependence is much stronger than predicted. Fluxes around 10^{-8} dpa/s possess incubation times of less than 1 dpa, while 10^{-6} dpa/s shows incubation delays of some 30 dpa. Experiments in commercial steel show a much weaker flux effect (i.e., more consistent with the magnitude of the simulated effect), with longer incubation times [1].

Finally, the terminal void density is shown in Fig. 8. This refers to clusters that should be 'visible' to TEM measurement, namely, those with radius $r > 0.5$ nm, for comparison with experimental measurements. The results differ from those shown in Fig. 7, Ref. [19], because of changes in both the numerical treatment and in the dislocation bias factors. The new results are in good agreement with experiment.

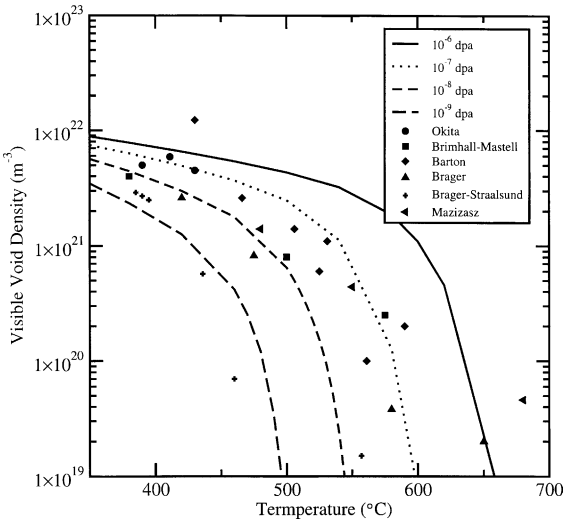

Fig. 8. Terminal density of visible voids (taken at 100 dpa total fluence) versus temperature for three irradiation dose rates, of 10^{-6}, 10^{-7}, and 10^{-8} dpa/s.

4. Conclusions

The predicted swelling behavior changes significantly when dislocation co-evolution is included along with void nucleation and growth. The crossover from incubation behavior to steady growth is more abrupt than when the dislocations are held constant. The simulations

still do not fully reproduce the behavior seen in commercial reactor steels. In part, this is because the model is appropriate only for high-purity rather than commercial alloys. The predicted temperature- and flux-dependent incubation time is qualitatively consistent with observations for high purity ternary steel. However, the available measurements suggest a stronger flux-dependence.

Once incubation is complete, the simulated quasi-steady-swelling rate is now more nearly constant with dose and shows a greatly reduced dependence on temperature and dose rate. The evolution in dislocation density from the solution-annealed starting point towards the terminal value is required to predict this more realistic swelling behavior. At most temperatures studied, the dislocation density increases from its solution-annealed starting values, along with the growing void sinks. This prolongs the period of steady swelling as compared to calculations with a fixed dislocation content.

On the other hand, the predicted terminal void density is similar whether a fixed or time-dependent dislocation density is used. This is because the stable voids nucleate very quickly in the simulation, before the dislocation density can change appreciably from its initial value. The predicted stable void density is also in good agreement with experiment.

These dislocation and void co-evolution calculations use time-independent (i.e., independent of the evolving dislocation density) dislocation bias factors. This is an approximation, since the bias factors will depend on the details of the local dislocation arrangement, including separation distance from nearby dislocation segments. The calculations appear to give good results for the terminal void densities. However, they underestimate the incubation times, even for experiments in high-purity steel.

Further, separate modeling of network and loop dislocation evolution may result in more realistic, time-dependent dislocation bias factors. Such an improved dislocation evolution model is planned for future work. It will also encompass irradiation phenomena like production bias [31], defect cluster mobility and coalescence and loop adsorption at network dislocations. Currently mobile interstitial clusters can be said to be approximated as if they have exactly the same mobility and bias factors as interstitial monomers [32].

Acknowledgments

This work was performed under the auspices of the US Department of Energy by the University of California, Lawrence Livermore National Laboratory under Contract No. W-7405-Eng-48. This research was funded by the Department of Energy's Nuclear Energy Research Initiative (NERI) Program through the Office of Nuclear Energy, Science, and Technology.

References

[1] F.A. GarnerNuclear Materials, vol. 10A, 1994, p. 419 (Chapter 6).
[2] F.A. Garner, M.B. Toloczko, B.H. Sencer, J. Nucl. Mater. 276 (2000) 123.
[3] T. Okita, T. Kamada, N. Sekimura, J. Nucl. Mater. 283–287 (2000) 220.
[4] T. Okita, Effect of dose rate on irradiation behavior in structural materials, Thesis, University of Tokyo, 2000.
[5] T. Okita, T. Sato, N. Sekimura, F.A. Garner, in: Proceedings of the Fourth Pacific Rim International Conference on Advanced Materials and Processing, vol. PRICM-4, 2001.
[6] T. Okita, T. Sato, N. Sekimura, F.A. Garner, L.R. Greenwood, W.G. Wolfer, in: Proceedings of the 10th International Symposium on Environmental Degradation of Materials in Nuclear Power Systems – Water Reactors, 2001.
[7] T. Okita, T. Sato, N. Sekimura, F.A. Garner, L.R. Greenwood, J. Nucl. Mater. 307–311 (2002) 322.
[8] A.D. Brailsford, R. Bullough, J. Nucl. Mater. 44 (1972) 121.
[9] J.L. Katz, H. Wiedersich, J. Chem. Phys. 55 (1971) 1414.
[10] K.C. Russell, Acta Metall. 26 (1978) 1615.
[11] H.L. Heinisch, J. Nucl. Mater. 103&104 (1981) 1325.
[12] H. Wiedersich, Radiat. Eff. 12 (1972) 111.
[13] T. Leffers, B.N. Singh, A.V. Volobuyev, V.V. Gann, Philos. Mag. A 53 (1986) 243.
[14] C.H. Woo, B.N. Singh, Philos. Mag. A 65 (1992) 880.
[15] C.H. Woo, B.N. Singh, F.A. Garner, J. Nucl. Mater. 191 (1992) 1224.
[16] C.H. Woo, J. Comput.-Aided Mater. Des. 6 (1999) 247.
[17] R. Bullough, B.L. Eyre, K. Krishnan, Proc. Royal Soc. London A 346 (1975) 81.
[18] M.P. Surh, J.B. Sturgeon, W.G. Wolfer, J. Nucl. Mater. 325 (2004) 44.
[19] M.F. Wehner, W.G. Wolfer, Philos. Mag. A 52 (1985) 189.
[20] W.G. Wolfer, L.K. Mansur, J.A. Sprague, in: M.L. Bleiberg, J.W. Bennet (Eds.), Proceeding of the International Conference on Radiation Effects in Breeder Reactor Structural Materials, vol. 2, 1977, p. 841.
[21] A.A. Semenov, C.H. Woo, Phys. Rev. B 66 (2002) 024118.
[22] N.M. Ghoniem, D.D. Cho, Phys. Status Solidi (a) 54 (1979) 171.
[23] N.M. Ghoniem, S. Sharafat, J. Nucl. Mater. 92 (1980) 121.
[24] K.C. Russell, Acta Metall. 19 (1971) 753.
[25] W.G. Wolfer, A. Si-Ahmed, Philos. Mag. A 46 (1982) 723.
[26] B.B. Glasgow, A. Si-Ahmed, W.G. Wolfer, F.A. Garner, J. Nucl. Mater. 103 (1981) 981.
[27] M.P. Surh, J.B. Sturgeon, W.G. Wolfer, J. Nucl. Mater. 328 (2004) 107.
[28] M.P. Surh, J.B. Sturgeon, W.G. Wolfer, in: M.L. Grossbeck, T.R. Allen, R.G. Lott, A.S. Kumar (Eds.), Effects of Radiation on Materials: 21st International Symposium, vol. ASTM STP 1447, 2003.
[29] W.G. Wolfer, B.B. Glasgow, Acta Metall. 33 (1985) 1997.
[30] L.K. Mansur, J. Nucl. Mater. 206 (1993) 306.
[31] C.H. Woo, A.A. Semenov, B.N. Singh, J. Nucl. Mater. 206 (1993) 170.
[32] T. Okita, W.G. Wolfer, J. Nucl. Mater. 327 (2004) 130, Appendix A.